

Anti-coherence based molecular electronics: XOR-gate response

Roi Baer¹ and Daniel Neuhauser²

¹*Institute of Chemistry and the Lise Meitner Minerva-Center for Quantum Chemistry, the Hebrew University of Jerusalem, Jerusalem 91904 Israel.*

²*Department of Chemistry, University of California, Los Angeles CA 90095-1569*

(Draft: Saturday, September 29, 2001)

Abstract: We point out and simulate the possible utility of anti-coherence in molecular electronics. In ballistic transfer through a molecule with a large loop that fulfils a certain phase condition on the loop structure, the transfer would be anti-coherent. By applying one or two control voltages to the molecule, that modify the relative phase through the two parts of the loop, the transfer could be controlled, just like in FET or in XOR gates. The simulations use the absorbing-potential based flux-flux formulae with a Huckel Hamiltonian in a Landauer formulation, and are numerically equivalent to a weighted time-dependent correlation function.

I. Introduction

The miniaturization of devices from silicon semiconductors toward single-molecules offers the possibilities of new paradigms for molecular devices¹⁻⁵. In particular, the miniaturization offers the possibility of using quantum effects^{6,7}.

In this article we explore the use of the most basic quantum effect, coherence, for computation. There have been some discussions of increased conductivity due to coherent transfer in molecules in which the electron can pass through two routes⁸. However, the opposite effect, anti-coherence, has generally been ignored in molecular devices.

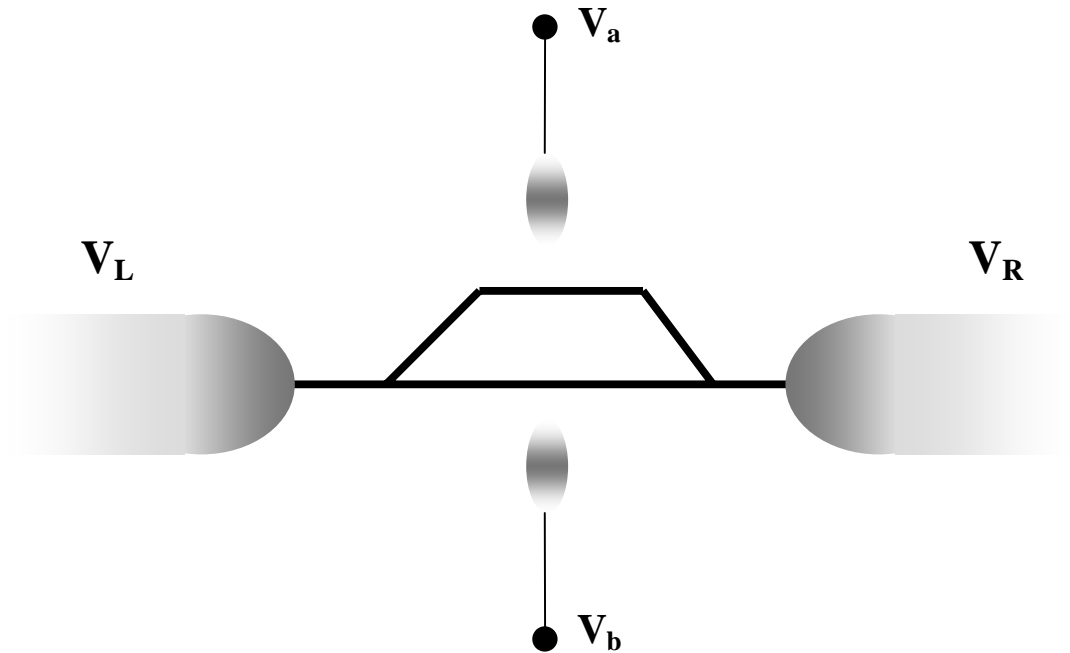


Figure 1: A schematics of a molecule with a loop which is capable of showing anti-coherent or coherent transfer, depending on the work functions of the leads (determining whether the transfer in the loop is ballistic or tunneling-like), and the control voltages on either side of the loop. With one control, a non-linear FET-like I-V curve results.

Anti-coherence is potentially very useful for small devices. For example, consider an electron going through a ring where the phase on one side cancels the phase on the other side (see Figure 1). Formally, and in the model calculations we show, the conductivity becomes extremely small. The molecule is then in an “off” state. By changing the phase through one of the rings, for example through voltage changes (as discussed below) the anti-coherence disappears, and the conductivity reverts to a large value (“on”). Thus, the ratio of conductivities between the “on” and “off” states would be quite large. This is to be contrasted with coherent transfer along the same-molecule, in which the phases of the electron going through the ring add up coherently. In that case, the conductivity increases by a factor of only 4 (i.e., 2^2) over the non-coherent value, and remains within the same order of magnitude. Notably, the same issues arise in optical communications where Mach-Zender and ring-oscillator modulators are used.

In a previous paper⁶, we have shown that, in model Huckel calculation, the anti-coherence effects are marked. In this paper we further investigate these effects.

For one, we show how anti-coherence can be used to establish a simple “XOR” gate. This gate is again made of a loop of unequal sides. Each side of the loop is now attached to a voltage gate, which, in our simple model, changes the potential of one of the atoms in the loop (an opposite one on each side of the loop). The XOR input signals are now the gate voltages and the XOR output is the current carried through the device. When the gate voltages are either both small or both large, corresponding to the input signals of 0-0 or 1-1, the current through the device is minute, i.e. the output value is 0. But when one is large and the other is small, corresponding to 0-1 or 1-0 inputs, the current through the device is large, yielding an output signal of value 1. Thus, the conductivity is an “XOR” as a function of the gate voltages. We demonstrate that this effect is obtained computationally, and is robust with respect to small voltage changes. Consequently, if just one of the parts of the loop is modified, then an FET transistor results – zero current when the bias is low and a high current when it is high.

For understanding our results in simple terms, we derive a simple rule for predicting the degree of anti-coherence in a molecule, in terms of the difference in loop-part length and Fermi-momentum.

A separate issue is the computational scheme used for deriving the results. Here we use absorbing potentials^{9,10} which are a very simple and robust approach to model the leads. There are two sub-approaches with absorbing potentials⁵. The first is a flux-flux based method¹¹ which has an advantage of simplicity and is analogous to self-energy methods^{12,13}. The second sub-approach using absorbing potentials would be the initial-value time-dependent method¹⁴⁻¹⁶. The initial-value approach is computationally powerful for these types of problems, since it scales linearly with the problem size. However, the problem sizes we consider are so small (less than 100 sites) so the most straightforward application of the flux-flux methods is sufficient.

The paper is specifically arranged as follows. We first discuss the loop system and its Huckel simulation. The methodology is also presented. This is followed by a qualitative discussion. We next discuss the computational results of the XOR, including contact ef-

fects (i.e., showing lack of qualitative contact effects). The concluding section considers methodological extensions and further effects that need to be simulated, including vibrational, self-consistent treatments and even correlation. We also mention the extension of this system, for example to a band-structure type as well as multiple-branches systems.

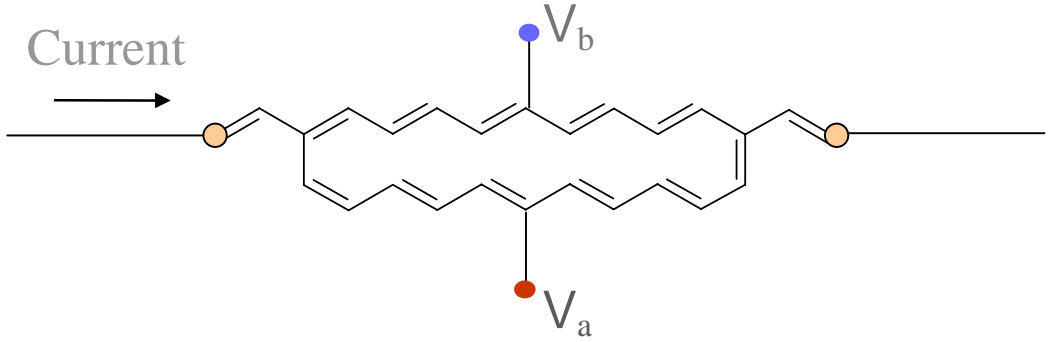


Figure 2: A schematic of the simulated system. The leads are coupled either weakly or strongly to the molecular wire. The two gate voltages V_a and V_b are variable.

II. Theory

A. System and Hamiltonian

The system is depicted in Figure 1 and Figure 2. It has six parts. Two leads connected to two wires, which bifurcate into two branches of the loop. In addition, there are the two gates on each of the two branches. The system is modeled with a Huckel-Hamiltonian,

$$\mathbf{H} = \sum_{i,j} (H)_{ij} a_i^+ a_j. \quad (1)$$

This 1-body Hamiltonian describes nearest-neighbor coupling $H_{\langle ij \rangle} = \beta_i$ ($\langle ij \rangle$ means that sites i and j are nearest neighbors), where in the wire β_i alternates between two values¹⁷

of β , -2.55eV and -2.85eV , to accommodate Peierls distortion along the wire. We also study the behavior of the system as a function of the coupling β parameter between the wire and the metal lead γ_{MW} , which takes on two values, $\gamma_{MW} = 2eV$ for a strong coupling and $\gamma_{MW} = 0.1eV$ for a weak coupling.

The diagonal part of the Hamiltonian is written as:

$$H_{ii} = \varepsilon_{i0} + Vv_i + V_a\delta_{i,a} + V_b\delta_{i,b} - i\Gamma_i. \quad (2)$$

Here, ε_{i0} , is the site i energy, taken to be -6.6 eV ¹⁷, corresponding to carbon-type sites and metals with similar intrinsic work function to carbon. Also included: an external voltage distribution v_i , derived from the potential difference V between the metallic leads; the gate voltages V_a and V_b , assumed to affect only one atom on each of the branches of the loop (atoms a and b). And finally, an absorbing potential, designed to simulate the infiniteness of the leads.

At the leads, the site-dependent voltage distribution is a number between $+0.5$ (on the left lead) and -0.5 (on the right lead). In this type of calculation, one must postulate the voltage distribution along the molecule. We have pursued two possibilities. One, where $v_i = 0$ within the wire, i.e., a molecule in which the voltage is nonzero only on the leads. The second choice, is a voltage drop which is a linear ramp, i.e. varying v_i between $+0.5$ and -0.5 linearly with the distance of atom i from the leads.

V_a , V_b , the gate voltages applied, respectively to each branch of the loop, are the input controls of the XOR gate. Their combined input determines the current flow from one lead to the other through the device. In this crude treatment we assume that these voltages each operate on a single site, denoted by a, b . We assume that the voltage gates are isolated from the molecule, and current cannot flow through them, see Figure 1. In a more realistic treatment, the effect of the gate voltage should extend over several sites, but this fact is not expected to change the qualitative effects we show subsequently, since the phase change would now increase to several sites. In practice, one approach for including a controllable bias would be to change the distance of a charged electronically-isolated group.

The last item in the diagonal energy is the negative imaginary (absorbing) potential, $-i\Gamma_i$. This term allows arrangement decoupling, so that the scattering problem is converted into a simple bound-state like problem, as shown in the equations below, without invoking a self-energy term. The absorbing potential is robust: the results are insensitive to its particular form or shape as long as it is sufficiently large as the ends of the leads (on the order of the typical electron kinetic energies) and falls down smoothly to zero within each lead towards the molecular wire. The absorbing potential should extend to a distance equal to 1-2 wavelengths, which is particularly easy for the problem we are considering since the relevant electron kinetic energy is the Fermi energy, so that the de-Broglie wavelengths are quite small ($\lambda_F \sim 4$ CC bond lengths). The potential is a parabolic absorbing potential; for example, the absorbing potential on the left lead (denoted by “L”) has the form

$$\Gamma_j^L = \Gamma_{\max} \left(1 - \frac{j}{\Delta j}\right)^2 \quad j \leq \Delta j, \quad (3)$$

and zero elsewhere, where we introduced the width of the absorbing potential (taken here as $\Delta j = 15$), and its maximum, $\Gamma_{\max} = 4\text{eV}$ here.

B. Methodology

From the Hamiltonian, we can compute the current through Landauer’s formula^{18,19}:

$$I = \frac{2e}{h} \int \Delta f(E) N_{LR}(E) dE, \quad (4)$$

where $N_{LR}(E)$ is the cumulative transmission probability (i.e. a summation on the transmission probabilities of all states of energy E) and

$$\Delta f(E) = f_L(E) - f_R(E), \quad (5)$$

where we introduce the Fermi-Dirac function, e.g.,

$$f_R(E) = \frac{1}{1 + \exp\left[\frac{(E - \mu_R)}{k_B T}\right]}, \quad (6)$$

with $\mu_R = \mu - eV/2$ and similarly $\mu_L = \mu + eV/2$, where V is the potential across the molecule, μ is the chemical potential of the leads and T is the temperature,.

The cumulative transmission probability can be calculated from an expression by Seideman and Miller¹¹:

$$N(E) = 4 \text{Tr}(G\Gamma_L G^* \Gamma_R). \quad (7)$$

where

$$G(E) = \frac{1}{E - H}. \quad (8)$$

Recall that H is an intrinsically complex matrix due to the absorbing potential. Note the similarity and differences with the familiar self-energy formulation^{12,19,20} in which the operators are energy-dependent. Here, Γ is an absorbing-potential, which is energy-independent. Further, the absorbing potential is applicable regardless of the specifics of the geometry of the channel. The absorbing potential does require modeling part of the leads, but it is only a small part since the de-Broglie wavelength is not too large for electrons near the Fermi energy. This trace formalism is very convenient, avoiding very detailed calculations that one is forced to make using for example scattering wavefunctions for every energy E ²¹.

Another, potentially important property of the absorbing-potential framework is that it can be recast rigorously in terms of a time-dependent correlation function with the resulting expression completely equivalent to Eqs. (4)-(7):

$$I = \frac{8e}{\pi\hbar^2} \text{Im} \int_0^\infty \text{tr} \{ \hat{\Phi} \hat{\Gamma}_L \hat{\Gamma}_R(t) \} dt \quad (9)$$

where the weight operator is:

$$\hat{\Phi} = \int \hat{G}(E) \Delta f(E) dE = \pi \frac{k_B T}{\hbar} \int_0^\infty \frac{e^{i\mu_R \tau/\hbar} - e^{i\mu_L \tau/\hbar}}{\text{sh}(\pi k_B T \tau/\hbar)} e^{-i\hat{H}\tau/\hbar} d\tau \quad (10)$$

The weight in Eq. (10) could be evaluated from a short-time Chebyshev approach²². The proof of Eqs. (9)-(10) is supplied in an upcoming paper.

Application of this formalism is appealing because of its simplicity. All that is required is the description of a relatively small part of the leads and the diagonalization of the complex-symmetric Hamiltonian,

$$H = U \varepsilon U^T, \quad (11)$$

in terms of which

$$I = \frac{16e}{h} \text{Re} \sum_{nm} \frac{\Phi_n}{\varepsilon_m^* - \varepsilon_n} \bar{\Gamma}_{L,nm} \bar{\Gamma}_{R,mn}, \quad (12)$$

where

$$\bar{\Gamma}_L = U^T \Gamma_L U, \quad (13)$$

and

$$\Phi_n = \int \frac{\Delta f(E)}{E - \varepsilon_n} dE. \quad (14)$$

This formalism is sufficient for 1-body Hamiltonians which can be readily diagonalized, i.e., with ~5000 basis functions. For larger size problems, or if coupling to other degrees of freedom is desired, an alternate time-dependent approach in which the Hamiltonian is not diagonalized but only propagated is possible, based either on Eqs. (9)-(10) or alternately on the initial-value problem with absorbing potentials.

C. *Qualitative Analysis*

It is easy to predict, on a semiclassical level, the expected current in the cross linked molecular wire. As long as the transfer in the wire is ballistic, the electron would develop, semiclassically, a phase of:

$$\phi = n\beta k, \quad (15)$$

upon going a distance of n-sites, where β is the typical nearest-neighbor coupling and k is the momentum of the electron. Since we typically deal with low voltages, k should be taken as the value, within the molecule, of the momentum near the Fermi-energy. Anti-coherence results when the phase difference is an odd integer (“2m+1”) multiple of π , i.e., when the path-difference between the two parts of the loop fulfils:

$$\beta k \delta n = (2m + 1)\pi . \quad (16)$$

For our specific simulation of a system in which the leads have the same work-function as the molecule (same Fermi energy), and using the fact that this Fermi-energy is exactly at the center of the spectrum of H , and therefore the system is at half-filling, we get

$$k = \frac{\pi}{2\beta} , \quad (17)$$

so the result is simply

$$\delta n = (4m + 2) = 2, 6, 10, \text{etc.} \quad (18)$$

A more compact derivation of this result is: at the Fermi momentum at half-filling, the Huckel wavefunction changes sign every second site. Thus, for anti-coherence, the two parts of the loop have to be different in length by two sites, or six sites, etc.

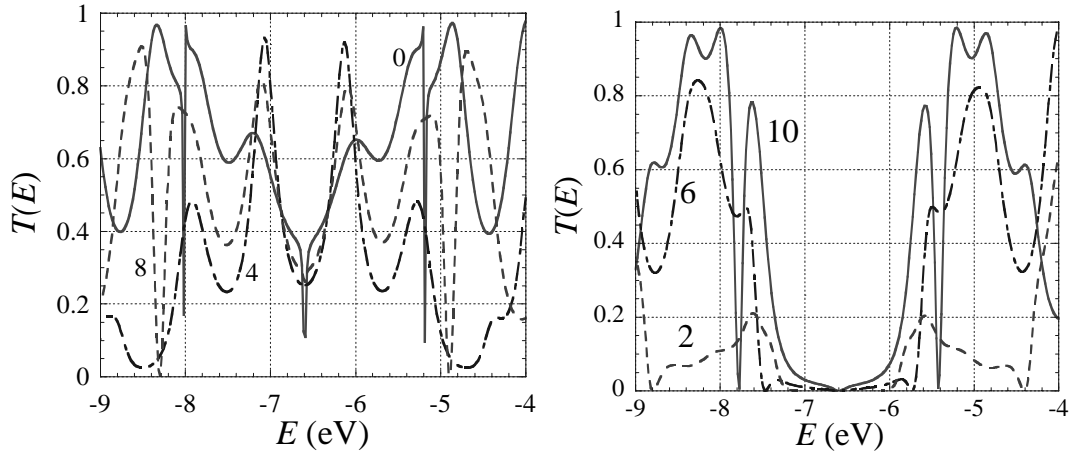


Figure 3: Transmittivity ($T(E)$) in the strong metal-molecule coupling, $\gamma_{WM} = 2\text{eV}$ for zero bias volt ages, as a function of the voltage, and keeping one branch of the loop 12 bonds long, showing : (a) coherent transfer in which the other side of the loop has 12, 8, and 4 bond (i.e., so the difference between the two loops is $\delta n = 0, 4, 8$ bonds), and (b) Anti-coherent transfer for loops with $\delta n = 2, 6, 10$. The labels in the figures refer to δn .

This discussion is semiclassical, in that we assume that we can associate a propagating phase and direction to the wavefunction. It is therefore not expected to be valid for very small systems, where the branches are smaller than a wavelength. For example, for meta-benzene, hooked to two sites, this discussion would predict an anti-coherence, but the

system site is too small (below a wavelength) to trust such a prediction. However, for larger systems the semiclassical consideration agrees with the Huckel prediction for the Hamiltonian.

III. Results

Below we show results of using Eqs. (4)-(7) or Eqs. (9)-(10). This problem is one-dimensional, so the cumulative probability $N(E)$ is the transmission $T(E)$. The leads and branches were chosen to be 20 and 12 bonds long, and one loop side was 12 bonds long, while the second was varied from having 12 bonds (i.e., $\delta n = 0$) to having 2 bonds. Room temperature was used; it is sufficiently low that it would be essentially the same as using zero temperature.

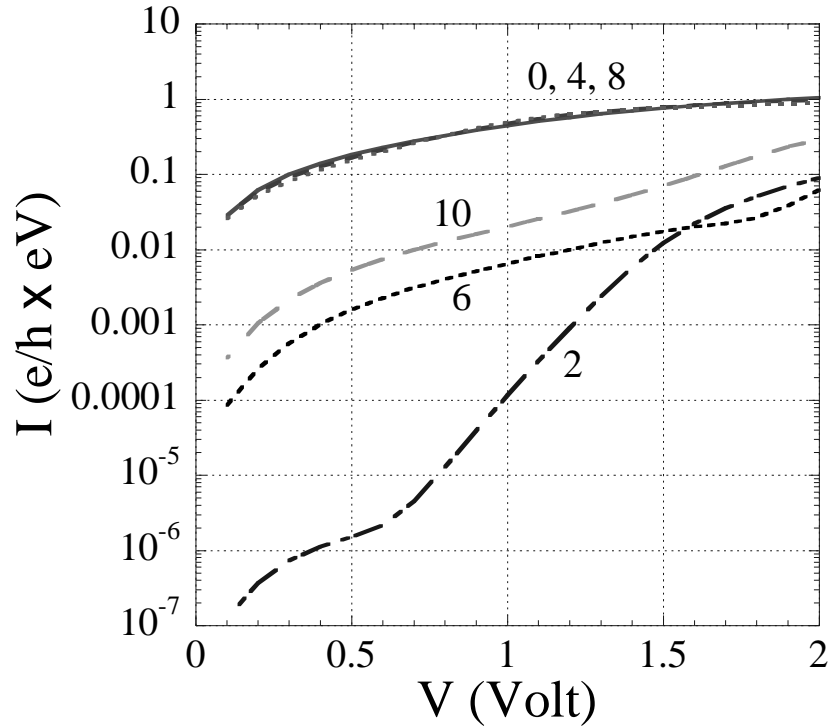


Figure 4: The $I - V$ relation for coherent ($\delta n = 0, 4, 8$) and anti-coherent ($\delta n = 2, 6, 10$) transfer through the Huckel system, as a function of δn . Strong coupling case, $\gamma_{MW} = 2eV$.

Figure 3 shows the transmittivity ($T(E)$) of the system, for zero bias voltage ($V_a = V_b = 0$) for several lengths of one branch of the loop. Note that the transmittivity is formally a

functional of voltage distribution, as the Hamiltonian is (although in practice is usually varies little with voltage in this type of treatments), and it is shown here for $V = 0$. The computations of the $I - V$ curves below do use the correct voltage-dependent transmittivities. The results were obtained for a metal-wire coupling $\gamma_{MW} = 2\text{eV}$. This is the strong interaction regime, comparable to the lead-branch contacts within the loop.

The figure shows, that for differences $\delta n = 0, 4, 8$ i.e. $4m$ (where m is an integer) bond lengths, and for differences of $\delta n = 2, 6, 10$, i.e. $4m+2$ bond lengths anti-coherence results. At higher (and lower) energies $T(E)$ oscillates, rising for the anti-coherent systems. This is because the electron momentum k gets farther from the Fermi momentum, so the anti-coherence along the two-branches is destroyed. Note that $T(E)$ stays flattest for a loop of $\delta n = 2$. Specifically, for k slightly removed from the Fermi momentum, the phase-difference $\delta\phi = \delta n \cdot \beta k$ deviates from $(2m + 1)\pi$ increasingly with δn .

Figure 4 shows the associated current-voltage relation. For the anti-coherent case, the voltage is initially flat due to the vanishing of $T(E)$ at small voltages, and then rises quickly. Again, the $I - V$ curve stays lowest for $\delta n = 2$.

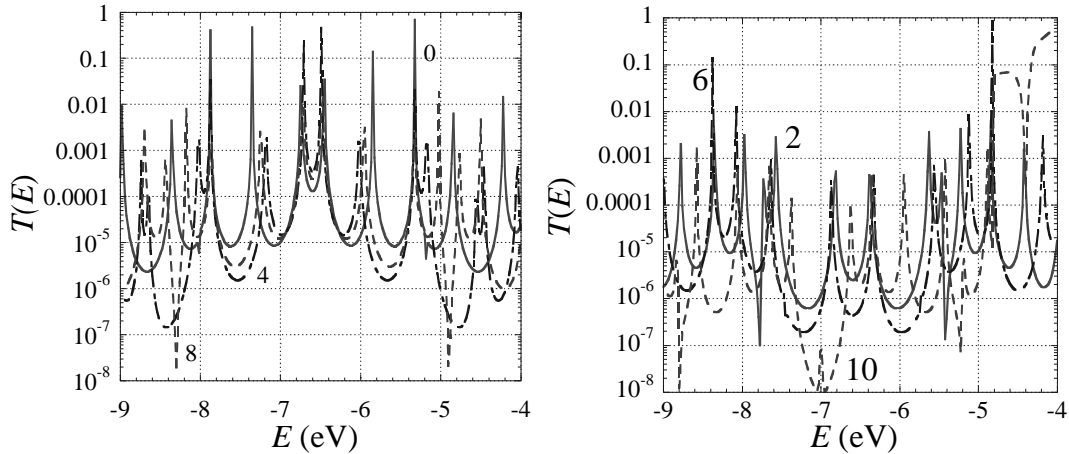


Figure 5: Transmittivity ($T(E)$) for a Huckel system. Similar to Figure 3, but for a weak metal-molecule coupling ($\gamma_{WM} = 0.1\text{eV}$), and using a log-scale.

Figures 5-6 are similar to 3-4 but for a weak metal-molecule interaction, $\gamma_{MW} = 0.1\text{eV}$. The $T(E)$ curve is now on a logarithmic scale, since the weak coupling turns the molecule into a resonator with well-spaced resonances where the interaction peaks. Still, the

$I - V$ curve in Figure 6 shows again that anti-coherence results if $\gamma_{MW} = 0.1\text{eV}$, i.e., a weak interaction. The anti-coherence results from the structure of the inner loop and is not related to the contacts. In reality, this would be true as long as the contacts are sufficiently far from the loop, i.e., the branches are sufficiently long.

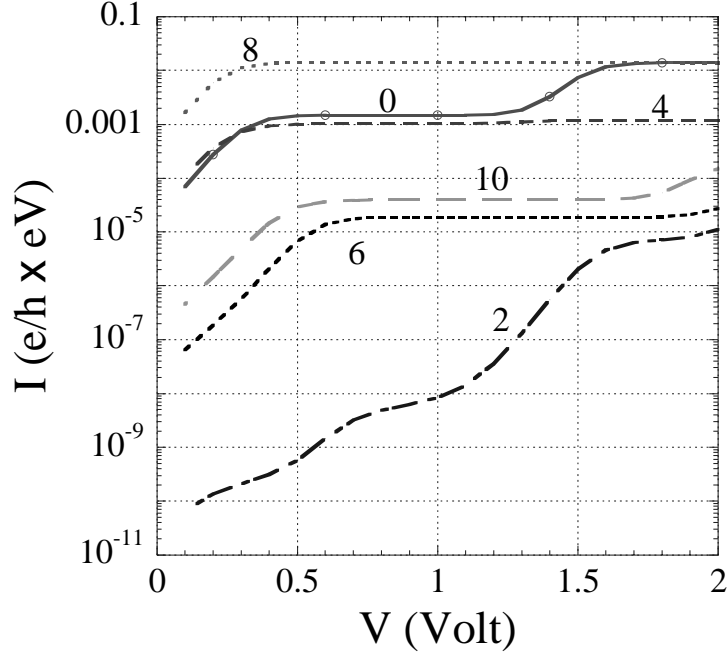


Figure 6: The $I - V$ curves for coherent and anti-coherent transfer through the Huckel system. Weak lead-wire coupling case, $\gamma_{MW} = 0.1\text{eV}$.

Next we turn to the “XOR”-function. Here it refers to the current in the leads. An ideal “XOR” gate in this case would be “OFF”, i.e., very small current, when the inputs in the leads are both “OFF” (0 Volt) or both “ON” (1 Volt) and is “ON” (high current) otherwise. In Figure 7 we show the effect on the $I - V$ curve of applying voltages of 0 and 1 Volt in tandem. It is evident that the device shows a “XOR” behavior. Specifically, Table I shows the currents at $V = 0.6$ Volt – it is shown to be two orders of magnitude smaller in the “OFF” state than in the “ON” state.

Figure 8 examines the sensitivity of the “XOR” function to changes in the bias voltage V_b for fixed V_a . The gate is seen to be insensitive to small changes in the voltages.

Finally, we have also verified that the “XOR”-function properties are completely persevered in the case of weak coupling, as shown in Figure 9 and Table II.

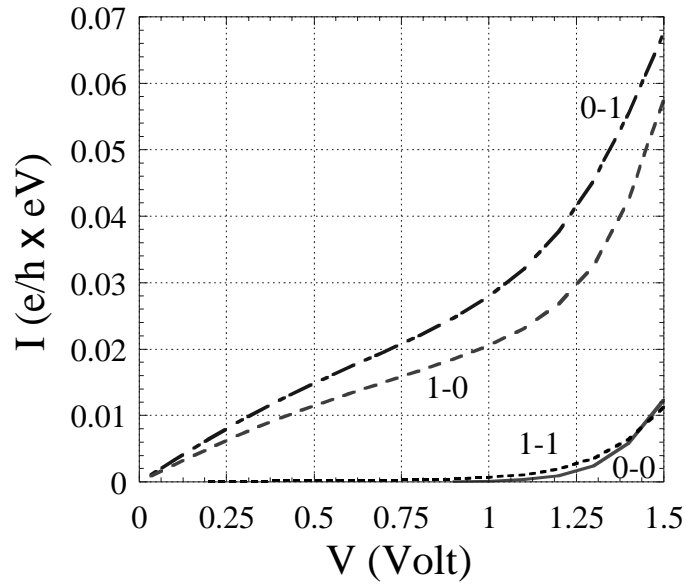


Figure 7: The effect on the $I - V$ curve of applying bias voltages of 0 and 1 Volt in tandem and separately.

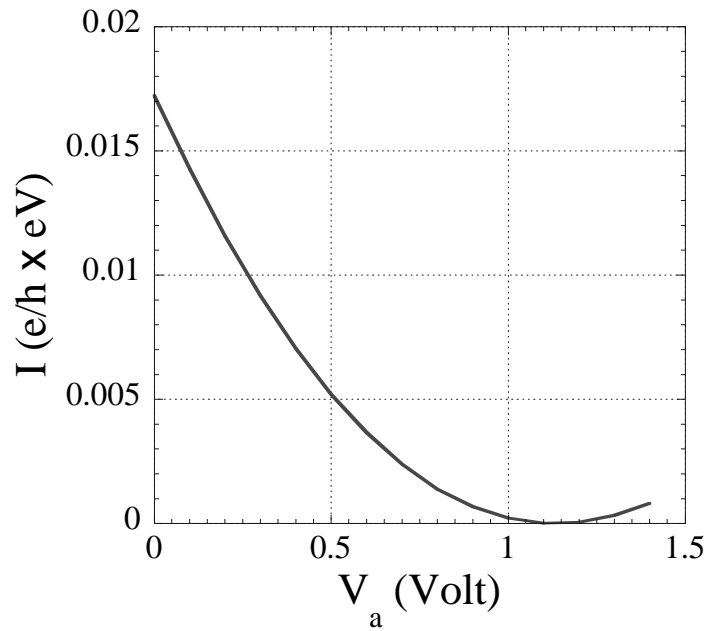


Figure 8: The sensitivity of the current (and therefore of the “XOR”) function to changes in the bias voltage V_b , fixing the other bias voltage and the voltage between the leads at $V_a = 1\text{Volt}$, $V = 0.6\text{Volt}$.

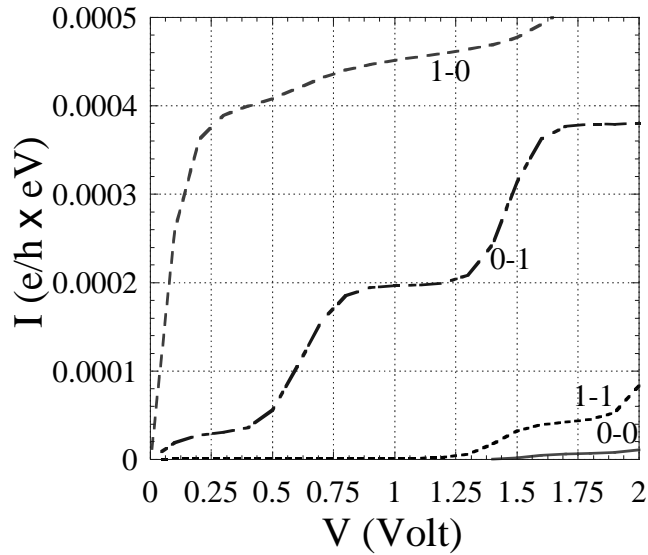


Figure 9: Similar to Figure 7, for weak-coupling, showing the preservation of the XOR-behavior then.

IV. Discussion

The results indicate that anti-coherence may be a very useful property of miniscule devices. Many open issues and further investigations remain.

- The Huckel Hamiltonian is very simplistic. Extended Huckel is a better choice and will be implemented in future simulations.
- Electron-interaction effects need to be included. The most important one here would be Coulomb charge distribution, so future studies would include a self-consistent treatment²⁰.
- Qualitatively, we can pre-estimate the polarization effects. The electron-density on either branch of the loop will be, without polarization, somewhat larger than the density on the right, “products” branch (since the electrons reach the end of the loop and get reflected). Once polarization is included, the electrons within the molecules would cause a slight charge migration within the molecule; however, for two similar size sides of the loop (different, e.g., only by $\delta n = 2$), the electron density would be expected to change essentially symmetrically, thereby preserving the anti-coherence effect.

- Vibrational effects may destroy the anti-coherence if they are too strong, just like they destroy coherence in quantum wires at high temperatures. The key is whether the anti-symmetric vibrations couple strongly enough to the electronic motion. Thereby, in practice molecules without strong coupling would be needed. Again, future studies would be used to estimate the effect.
- Ballistic conductance was recently measured in nanotubes²³. In a future study we will discuss the effects outlined here in nanotube systems.
- Here we concentrated on a single simple loop. Multiple loop systems are the next option. Consecutive loops, as depicted in Figure 9, would give an adjustable band-structure. As a speculation, one can imagine placing the shorter part of the loops in a specific chemical environment, and the longer part in another environment (for example by placing such molecules in two-sided membranes) thereby controlling the voltages on each side on each molecule simultaneously (and independent of the other side).
- More complicated loops (Figure 10) would offer the possibility of multiple terminals on the same compact molecule.
- Experimentally, other molecules with a loop structure may prove easier to work with. The key would be to work with molecules which fulfill relation (16). This can be accomplished by ensuring that the loop size is sufficiently small (but non-zero) and precisely set (as in the example here, of $\delta n = 2$). Alternately, a larger spread in the physical length-difference within the loop may be used if the Fermi-momentum is lowered, as can be achieved by working with other types of leads.
- The key to anti-coherence is to have ballistic motion. If the transfer was by tunneling, then the electron wavefunction would not pick a phase and the result of the loop would be a coherent (but tunneling, i.e., low intensity) transfer. This raises an interesting possibility: by changing the leads work function, the same molecule can be induced to alter its transfer from anti-coherent to coherent, or vice-versa. Even a completely symmetric loop, which would have coherent transfer naturally, can be induced

to have an XOR behavior by adding a fixed voltage and then varying the bias voltages.

- Similar coherent and anti-coherent effects would be observed also if the current is replaced by an electron from photoexcitation. In fact, even clearer effects would be seen since the electron could have high energy selectivity so there would be no Landauer's integral.
- The control can also be exercised by changing acidity⁴ rather than a change in voltage.

In conclusion, our simulations indicate that molecules with loops may be induced to yield a Young-experiment type behavior, when the condition in Eq. (19) is fulfilled. By changing the phase, logical gates such as "XOR" can be implemented. Since the current is a sensitive function of the gate potentials, it should be possible to quickly turn it on or off, thereby modulating the charge transport molecule. Thus, such molecules can act as fast modulators or switches.

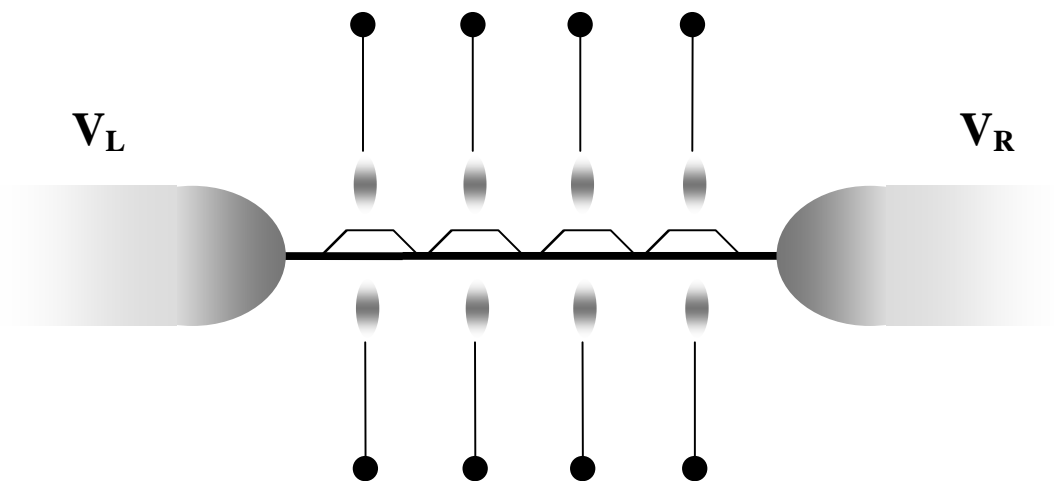


Figure 10: Schematics of an anti-coherence-controlled band-gap system obtained by consecutively placing several molecules containing loops. The voltages on the loop can be calibrated separately or the same voltage can be shared by each side of the loop.

Acknowledgements

We thank Mark Ratner, Jeffrey Zink, Eran Rabani and Abraham Nitzan for useful discussions or comments on the manuscript. Special thanks are due to Jim Heath for suggesting we check the application of this effect to XOR-gates. This work was supported by the National Science Foundation the Petroleum Research Fund and the Israel-USA Binational Foundation, grant no. 1998108.

Tables:

Table I: The current for a fixed voltage ($V = 0.6\text{Volt}$) for several bias voltages, showing an XOR-type behavior, for a strong wire-metal coupling.

V_a (Volt)	V_b (Volt)	$I\left(10^{-2} \frac{e \cdot eV}{h}\right)$
0	0	0.00
0	1	1.33
1	0	1.72
1	1	0.02

Table II: Similar to Table I, for a weak wire-metal coupling (and $V = 0.8\text{ Volt}$).

V_a (Volt)	V_b (Volt)	$I\left(10^{-4} \frac{e \cdot eV}{h}\right)$
0	0	0.00
0	1	1.85
1	0	4.40
1	1	0.01

References

- ¹ J. Jortner and M. Ratner, *Molecular Electronics*. (Blackwell Science Inc, 1997).
- ² A. Aviram and M. Ratner, *Molecular Electronics*. (New York Academy of Sciences, New York, 1998).
- ³ J. M. Tour, M. Kozaki, and J. M. Seminario, *J. Am. Chem. Soc.* **120** (9), 8486 (1998).
- ⁴ C. P. Collier, E. W. Wong, M. Belohradsky, F. M. Raymo, J. F. Stoddart, P. J. Kuekes, R. S. Williams, and J. R. Heath, *Science* **285** (5426), 391 (1999).
- ⁵ A. Nitzan, *Annu. Rev. Phys. Chem.* **52**, 681 (2001).
- ⁶ R. Baer and D. Neuhauser, submitted (2001).
- ⁷ C. Joachim, J. K. Gimzewski, and A. Aviram, *Nature* **408** (6812), 541 (2000).
- ⁸ M. Magoga and C. Joachim, *Phys. Rev. B* **59** (24), 16011 (1999).
- ⁹ D. Neuhauser and M. Baer, *J. Chem. Phys.* **92** (6), 3419 (1990).
- ¹⁰ D. Neuhauser and M. Baer, *J. Phys. Chem.* **94** (1), 185 (1990).
- ¹¹ T. Seideman and W. H. Miller, *J. Chem. Phys.* **96** (6), 4412 (1992).
- ¹² V. Mujica, M. Kemp, A. Roitberg, and M. Ratner, *J. Chem. Phys.* **104** (18), 7296 (1996).
- ¹³ L. E. Hall, J. R. Reimers, N. S. Hush, and K. Silverbrook, *J. Chem. Phys.* **112** (3), 1510 (2000).
- ¹⁴ R. Kosloff, *J. Phys. Chem.* **92** (8), 2087 (1988).
- ¹⁵ D. Neuhauser and M. Baer, *J. Chem. Phys.* **90** (8), 4351 (1989).
- ¹⁶ D. Neuhauser, M. Baer, R. S. Judson, and D. J. Kouri, *Comput. Phys. Commun.* **63** (1-3), 460 (1991).
- ¹⁷ P. J. Lowe, *Quantum Chemistry*, 2 ed. (Harcourt Brace & Company, New York, 1997).
- ¹⁸ R. Landauer, *Philos. Mag.* **21**, 863 (1970).
- ¹⁹ S. Datta, *Electronic Transport in Mesoscopic Systems*. (Cambridge University Press, Cambridge, 1995).
- ²⁰ S. N. Yaliraki, A. E. Roitberg, C. Gonzalez, V. Mujica, and M. A. Ratner, *J. Chem. Phys.* **111** (15), 6997 (1999).
- ²¹ E. G. Emberly and G. Kirczenow, *Phys. Rev. B* **58** (16), 10911 (1998).
- ²² R. Baer, Y. Zeiri, and R. Kosloff, *Phys. Rev. B* **54** (8), R5287 (1996).
- ²³ S. Frank, P. Poncharal, Z. L. Wang, and W. A. de Heer, *Science* **280** (5370), 1744 (1998).